RESEARCH PAPERS

Acta Cryst. (1998). D**54**, 711–717

Structure of 3,4-Dichloroisocoumarin-Inhibited Factor D

L. Brent Cole,† J. Michael Kilpatrick, Naiming Chu and Y. Sudhakar Babu*

BioCryst Pharmaceuticals, Inc., 2190 Parkway Lake Drive, Birmingham, AL 35244-2812, USA.
E-mail: babu@biocryst.com

(*Received 3 April 1997; accepted 22 July 1997*)

Abstract

Factor D (**D**) is a serine protease essential in the activation of the alternative complement pathway. Only a few of the common serine protease inhibitors inhibit **D**, binding covalently to the serine hydroxyl of the catalytic triad. 3,4-Dichloroisocoumarin (DCI) is a mechanism-based inhibitor which inhibits most serine proteases and many esterases, including **D**. The structure of the enzyme:inhibitor covalent adduct of **D** with DCI, **DCI:D**, to a resolution of 1.8 Å is described, which represents the first structural analysis of **D** with a mechanism-based inhibitor. The side chain of the ring-opened DCI moiety of the protein adduct undergoes chemical modification in the buffered solution, resulting in the formation of an α-hydroxy acid moiety through the nucleophilic substitution of both Cl atoms. The inhibited enzyme is similar in overall structure to the native enzyme, as well as to a variety of isocoumarin-inhibited trypsin and porcine pancreatic elastase (PPE) structures, yet notable differences are observed in the active site and binding mode of these small-molecule inhibitors. One region of the active site (residues 189–195) is relatively conserved between factor D, trypsin, and elastase with respect to amino-acid sequence and to conformation. Another region (residues 214–220) reflects the amino-acid substitutions and conformational flexibility between these enzymes. The carbonyl O atom of the DCI moiety was found to be oriented away from the oxyanion hole, which greatly contributes to the stability of the **DCI:D** adduct. The comparisons of the active sites between native factor D, DCI-inhibited factor D, and various inhibited trypsin and elastase (PPE) molecules are providing the chemical bases directing the design of novel, small-molecule pharmaceutical agents capable of modulating the alternative complement pathway.

1. Abbreviations

D, factor D; **B**, factor B; DCI, 3,4-dichloroisocoumarin; DFP, diisopropyl fluorophosphate; DIP, diisopropyl phosphoryl moiety; **DCI:D**, covalent adduct of **D** with 3,4-dichloroisocoumarin, **DIP:D**, covalent adduct of **D** with diisopropyl fluorophosphate; PPE, porcine pancreative elastase; 5CL, [1-(5-chloro-4-oxo-4H-3,1-benzoxazin-2-yl)-2-methyl-propyl] carbamic acid 1,1-dimethylethyl ester. Bold print is used to signify complement proteins and adducts with them. The chymotrypsin numbering system is used for these serine proteases, accounting for insertions and deletions. 1dfp, Protein Data Bank code for **DIP:D** structure; 1dsu, Protein Data Bank code for native factor D structure; 1inc, Protein Data Bank code for 5CL:PPE structure.

2. Introduction

The activation of complement results in the expression of key host defense functions, executed through a series of enzymatic amplification steps. Factor D is the serum serine protease which catalyzes the enzymatic reaction required for the formation of C3-convertase in the alternative pathway of complement activation. This pivotal enzyme is unique among serine proteases in the fact that it does not require proteolytic cleavage in order to become enzymatically active (Lesavre & Muller-Eberhard, 1978), nor does it require an inhibitor for its inactivation. Tight regulation is maintained through high enzymatic specificity, low circulating concentration levels, and a purported conformational change in the active-site region. **D** has been determined to be the limiting enzyme in the cascading sequence of the alternative pathway (Lesavre & Muller-Eberhard, 1978). Although complement is one of the key effector mechamisms of host defense responding to infection or injury, inappropriate activation of complement may result in medical complications. Complement activation has been implicated in the inflammatory reactions which accompany myocardial infarction (heart attack), adult respiratory distress syndrome (ARDS), and post-heart-attack reperfusion injury (Yasuda *et al.*, 1990; Hansson *et al.*, 1989; Cryer *et al.*, 1989). As a result of its position as the limiting enzyme in the alternative complement pathway, **D** is the rational choice for pharmacological control of complement activation.

† Current address: Abbott Laboratories, Diagnostics Division, PO Box 152020, 1921 Hurd Drive, Irving, TX 75015-2020, USA.

Table 1. *Intensity data-collection and refinement statistics for* ***DCI:D***

Resolution (Å)	1.8
Number of crystals	1
Number of observations	163135
Number of unique reflections	18850
% Completeness	92.0
Merging *XENGEN R* factor (%)	9.0
Number of reflections used in *X-PLOR* refinement (8–1.8 Å, $I>2\sigma$)	16298
Number of protein atoms	1712
Number of inhibitor atoms	14
Number of water molecules	115
R factor	0.182
R free	0.251
R.m.s. deviation from ideal bond lengths (Å)	0.009
R.m.s. deviation from ideal bond angles ( )	1.5
R.m.s. deviation from ideal dihedral angles ( )	26.6
R.m.s. deviation from ideal improper dihedral angles ( )	1.3

Factor D is a 24 kDa single polypeptide chain which exhibits a high degree of amino-acid sequence identity with a variety of serine proteases, including pancreatic bovine trypsin, chymotrypsin A, human neutrophil clastase, porcine elastase, and rat mast cell protease (Niemann *et al.*, 1984). **D** has only one known natural substrate, cleaving a single arginyl–lysyl bond of factor B, once **B** is in the Mg^{2+}-dependent complex C3bB (Lesavre *et al.*, 1979). In comparison with other serine proteases, **D** has very low catalytic activity against synthetic ester substrates (Kam *et al.*, 1987), can be completely inactivated by relatively high concentrations of diisopropyl fluorophosphate, (Fearon *et al.*, 1974) and reacts moderately well with isocoumarin inhibitors (Kam *et al.*, 1992). The inhibition of **D** with 3,4-dichloroisocoumarin is the focus of this paper. In serum, **D** circulates at the lowest concentration of all complement proteins, 1.8 ± 0.4 μg ml^{-1} (Barnum *et al.*, 1984) as a potentially active protein (not as zymogen), yet is devoid of proteolytic activity against uncomplexed **B**. Thus, early proposals suggested that a conformational change is induced in **B** upon binding to **C3b** (Lesavre & Muller-Eberhard, 1978). Resulting from the low catalytic activity of **D** toward thioester substrates, others postulated that a conformational change in the active site of **D** may be induced by the substrate, the C3bB complex (Kam *et al.*, 1987). The structure of native **D** has been solved to 2.0 Å resolution (1dsu; Narayana *et al.*, 1994), demonstrating that the protein exhibits the same general structural fold as the serine protease superfamily, yet the catalytic triad residues are not positioned in a manner conducive to efficient catalysis, revealing a 'zymogen-like' conformation of the native enzyme. At minimum, a conformational change that realigns these residues must occur to induce enzymatic activity.

The first structure of **D** in an inhibited state has been published recently (1dfp; Cole *et al.*, 1997), comparing and contrasting the differences in the architecture of the respective active-site residues of **DIP:D**, the native enzyme, and DIP-trypsin. The techniques of structure-based drug design (reviewed by Bugg *et al.*, 1993) are currently being applied in the design of novel small-molecule inhibitors of this pivotal enzyme in complement activation. Isocoumarins are general mechanism-based inhibitors of many serine peptidases (reviewed by Powers & Kam, 1994), and one of the few potent inhibitors of D. To gain insight into the specificity and function of the active site of this unique serine protease, we crystallized **D** which had been completely inactivated by covalent modification with 3,4-dichloroisocoumarin (**DCI**). Here we report the structure of the enzyme: inhibitor adduct, **DCI:D**, to a resolution of 1.8 Å.

3. Experimental

3.1. *Crystallization*

Recently purified **D** (Volanakis & Macon, 1987) was dialyzed exhaustively against 10 m*M* Tris buffer, pH = 7.0, 100 m*M* NaCl, then concentrated to 10 mg ml^{-1}. To 18 μl of this protein solution, 2 μl of a 50 m*M* 3,4-dichloroisocoumarin [in dimethyl sulfoxide (DMSO)] solution was added, yielding a final concentration of 5 m*M* of the inhibitor (approximately a 12:1 ratio of inhibitor:enzyme). The solution was allowed to incubate for 4 h at room temperature before crytallization trials were begun. Hemolytic assays (Volanakis *et al.*, 1993) were conducted using the DCI-treated **D**, confirming 99% inhibition of the protein. One block-shaped crystal ($0.4 \times 0.2 \times 0.2$ mm) was grown by hanging-drop vapor diffusion against a well solution of 50 m*M* MES, pH = 5.6, 20% polyethylene glycol 6000, 0.2 *M* NaCl. The small crystal was visible at high magnification after 1 d, although the crystal was allowed to reach maximum growth after several days. X-ray diffraction data collection was initiated 14 d after the crystallization trials were set up.

3.2. *Enzyme inhibition*

In order to verify that the enzyme remained completely inhibited throughout the crystallization process, the half-life of the **DCI:D** adduct was investigated. A modification of the procedure previously described for determining deacylaytion was utilized (Kerrigan *et al.*, 1995). **D**, 1 μ*M*, as allowed to react with DCI, 50 μ*M*, for 0.5 to 1 h at room temperature. **DCI:D** complexes were separated from free DCI by centrifugation through a Bio-Spin 6 column (BioRad, Hercules, CA) as per the manufacturers suggestions. 50 μl of the eluate was diluted in either 1 ml of the 0.1 *M* HEPES, 0.5 *M* NaCl, pH 7.5 or 0.05 *M* MES, pH 5.8 and incubated at room temperature. Every hour aliquots were removed and added to a tenfold excess volume of 900 μ*M* substrate, and the enzymatic activity determined spectrophotometrically. Enzyme activity was compared

to **D**, without DCI, treated identically before and after centrifugation, and for each hour afterwards. From these data we were able to calculated the half-lives of the protein–drug complex. At pH = 7.5, the half-life of the acylated enzyme as determined to be 177 h, while at pH 5.8 (nearest the crystallization conditions) the half-life could not be determined, as no loss of inhibition was found over the duration of the experiment. The apparent rate of inhibition of factor D by DCI was determined under pseudo first-order conditions (Salvesen & Nagase, 1989). 50-fold molar excess of DCI was added to **D**, 1 or 2 μ*M*, in 0.1 *M* HEPES, 0.5 *M* NaCl, 10% DMSO, pH 7.5 at room temperature. 20 μl aliquots were withdrawn every minute, added to a tenfold excess volume of 900 μ*M* substrate, and the remaining enzymatic activity determined spectrophotometrically in an Anthos Labtec HT2 plate reader. Under these conditions we found an apparent rate constant of $40 \pm 4.16\ M^{-1}\ s^{-1}$. This is similar, although slightly lower than, the second-order rate constant of $190\ M^{-1}\ s^{-1}$ reported for DCI and **D** (Kam *et al.*, 1992).

3.3. *Data collection*

The enzyme crystallizes in space group $P2_1$, with unit-cell dimensions $a = 56.3$, $b = 51.7$, $c = 39.8$ Å, $\beta = 106.1°$. The asymmetric unit consists of a single molecule, unlike the native and **DIP:D** enzymes, which crytallized as dimers. Intensity data to 1.8 Å resolution were collected on a Siemens Xentronics multiwire area detector mounted on a Rigaku RU-200 rotating-anode X-ray generator (40 kV, 100 mA) for 8 d at room temperature. Data intensities were strong throughout the data collection. The data were processed and scaled using the *XENGEN* suite of programs (Howard *et al.*, 1987). Data-collection statistics are recorded in Table 1.

3.4. *Structure refinement*

Initial phases were obtained by the method of molecular replacement as implemented in *X-PLOR* (Brünger, 1990, 1992*a*). The search model was based upon the atomic coordinates of one monomer of the **DIP:D** structure. Initially, a partially complete intensity data set, 15.0–4.0 Å, was collected from a single crystal and used in the rotation and translation searches. Correct placement of the molecule in the unit cell was straightforward. The top peak from the rotation search was 11.1σ above the mean, with the next highest peak at 5.8σ. The rotated monomer was then translated into the unit cell, followed by a final translation search solution (6.4σ above the mean), resulting in a conventional crystallographic *R* factor of 0.397. Subsequent rigid-body refinement in *X-PLOR* lowered the *R* factor to 0.348 for 15.0–4.0 Å data. Following one cycle of energy minimization in *X-PLOR* (the *R* factor dropped to 0.247 for 6.0–2.5 Å data), electron-density maps were generated from calculated phases based on the roughly refined model using the Fourier coefficients $2F_{obs} - F_{calc}$ and $F_{obs} - F_{calc}$; these revealed clear density for the majority of the protein. Strong density from the benzoyl moiety of the covalently bound adduct was observed extending from the hydroxyl O atom of the active-site serine residue. Additional data were collected, processed, and merged to yield the final data set represented in Table 1. Iterative cycles of simulated annealing with molecular dynamics using *X-PLOR* (beginning temperature of 3000 K; slow-cooled to 300 K in 25 K steps after every 50 dynamic steps; 0.5 fs per step) followed by visual model rebuilding using the program *FRODO* (Jones, 1978) were conducted. Two loop regions in the molecule exhibited significantly broken density (residues Leu59 to Gly62 and Arg170 to Ala175). Both regions are solvent exposed, and were subjected numerous times thoughout the refinement to simulated-annealing omit map calculations in *X-PLOR* ($2F_{obs} - F_{calc}$ and $F_{obs} - F_{calc}$ omit maps were calculated), yet improved only slightly. The Leu59–Gly62 loop region is poor in all previously discussed **D** structures determined thus far, while the Arg170–Ala175 region is less well defined in this stucture. After comparing the packing interactions of the latter region in the native **D** and the **DIP:D** structures with the title structure, it was clear that the symmetry-related molecules were packed less densely in the **DCI:D** structure than in the two previously reported structures. Refinement of the structure of the protein continued as the resolution range was extended to include 8.0–2.0 Å data. Solvent and the benzoyl moiety of the 3,4-dichloroisocoumarin molecule were added to the coordinate set at this point, followed by several additional cycles of

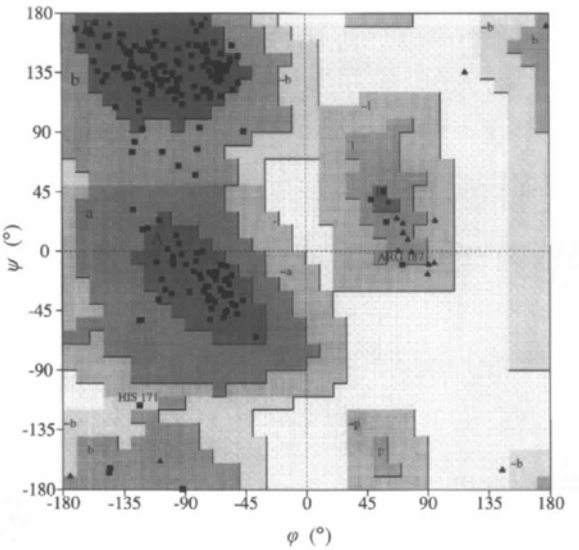

Fig. 1. Ramachandran plot for the main-chain torsion angle (φ, ψ) of the final **DCI:D** model from *PROCHECK*. Glycine residues are shown as triangles and all other residues are squares.

refinement. Midway through the refinement process, it was decided to create a test data set (10% of data excluded from working data set) in order to utilize free R values, or R_{free} (Brünger, 1992*b*). Provided the beginning temperature is sufficiently high in the simulated-annealing refinement, the free R value yielded appears to reproduce the value which would have been obtained *a priori* (Kleywegt & Brünger, 1996). Subsequent rounds of simulated annealing and energy minimization were run, with a beginning temperature of 4000 K and slow-cooled to 300 K (as carried out previously). Data were included to extend the resolution of the refinement from 8.0 to 1.8 Å. The quality of the refinement of **DCI:D** enzyme has been evaluated by *PROCHECK* (Laskowksi *et al.*, 1993). The Ramachandran plot (Fig. 1) identifies residues His171 and Arg187 to be in disallowed regions. Residue His171 is located in one of the disordered loop regions. The main-chain density is broken, yet the imidazole ring density is good. Residue Arg187 extends into solvent, with clear main-chain density and side-chain density through Cγ as well. Overall, the main-chain and side-chain parameters are indicative of a well refined structue.

4. Results and discussion

4.1. *General structure of the enzyme:inhibitor adduct*

The general architecture of the **DCI:D** adduct is very similar to that of the **DIP:D** inhibited enzyme and the native enzyme when examining the Cα tracing of the three protein structures. The single molecule retains the overall ellipsoidal shape of the two primarily β-sheet domains, concluding in an extended C-terminal helix, as is common in the serine protease family. The four disulfide bridges are consistent with the previously described structures. No significant changes are observed in the positioning of key active-site residue side chains when comparing **DCI:D** with **DIP:D** (Cole, unpublished results). The solvent molecules located are well ordered in the active-site region as well as those near the accessible surface of the protein. No significant solvent–inhibitor interactions were noted, thus the solvent structure has been removed from the figures for clarity. From the solid surface curvature model (Fig. 2), it can be seen that the main-chain backbone (including the exposed side chains of these peptides) surrounding the active site of the enzyme arches significantly upwards (as viewed), creating a rather deep narrow pocket (Nicholls *et al.*, 1991). This surface curvature is directly related to the accessibility of a given point on the protein surface to a water molecule. It then becomes clear as to how effectively the DCI moiety fills the majority of the accessible volume of the active site of **D**. A most noticeable feature is seen as the carbonyl O atom of the acylated inhibitor is positioned away from the oxyanion hole of the enzyme, forming a long hydrogen bond with the peptide amide N atom of Gly216 (3.4 Å). This orientation should make a strong contribution to the near irreversibility of the binding of DCI to **D**, as the half-life of the **DCI:D** adduct at pH 5.8 could not be determined since no enzymatic activity was regained. Instead, one carboxylate O atom of the side chain of the inhibitor was able to form a hydrogen bond (2.9 Å), to the peptide amide N atom of Gly193 in the oxyanion hole. The N atom of residue Ser195 does not have any hydrogen-bonding interactions.

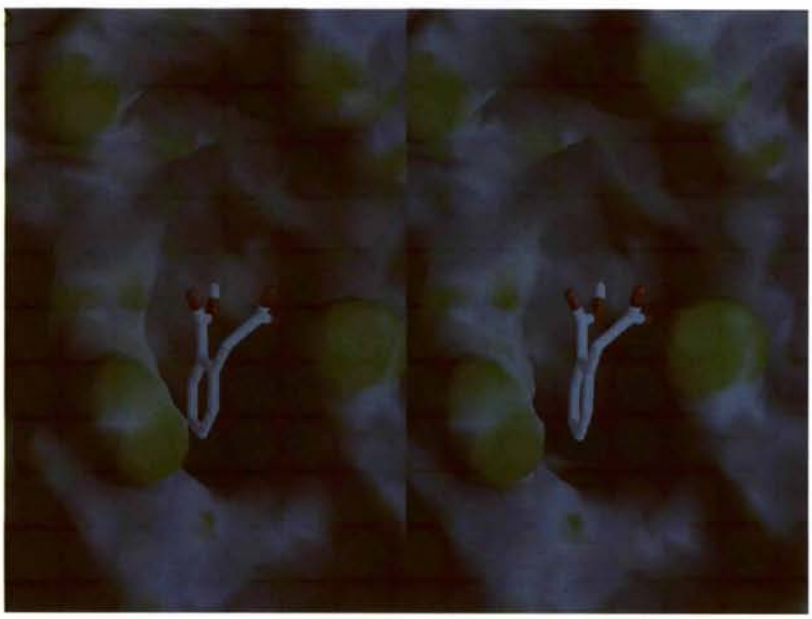

Fig. 2. Surface curvature diagram (describing the accessibility of water to the surface of the protein) of the active site of the **DCI:D** structure, created using *GRASP* (Nicholls *et al.*, 1991).

4.2. *Comparison of* ***DCI:D*** *with an isocoumarin–trypsin complex*

The crystal structure of trypsin, covalently bound to 4-chloro-3-ethoxy-7-guanidino-isocoumarin, has been chosen as a comparative model demonstrating the different small-molecule inhibitor-binding modes available to trypsin and to **D** (Chow *et al.*, 1990). In the aforementioned work, this substituted isocoumarin displays both a mono- and di-covalently linked binding modes with trypsin. The first mode of binding is very similar to that observed in the **DCI:D** adduct (Fig. 3*a*). The most noticeable difference is the position of the protein backbones along residues 213–218 (left side as viewed). The second set of strands shown (residues 188–196, right side as viewed) are virtually identical in most of the serine protease superfamily. The respective active-site Ser195 and Asp102 residues nearly overlap, while the His57 positions differ significantly. (The rationale for this difference has been discussed extensively in previous factor D papers: Cole *et al.*, 1997; Narayana *et al.*, 1994.) In this first binding mode, the aromatic rings of the two inhibitor molecules are almost superposed, though it quickly becomes evident that the **DCI:D** binding site could not accommodate the 7-guanidino group (of the isocoumarin inhibitor) inside the *S*1 specificity pocket without breaking the Arg218–Asp189 salt bridge at the bottom of the specificity

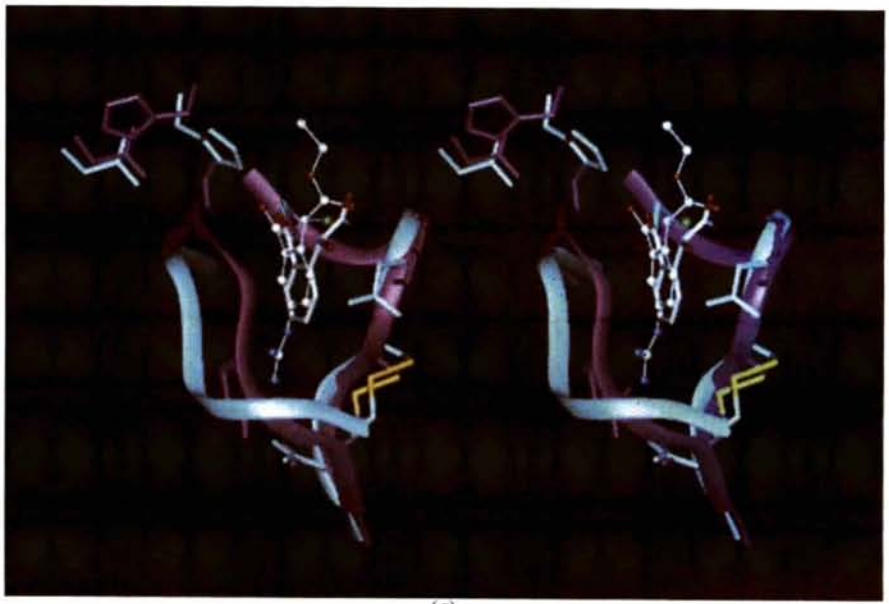

(*a*)

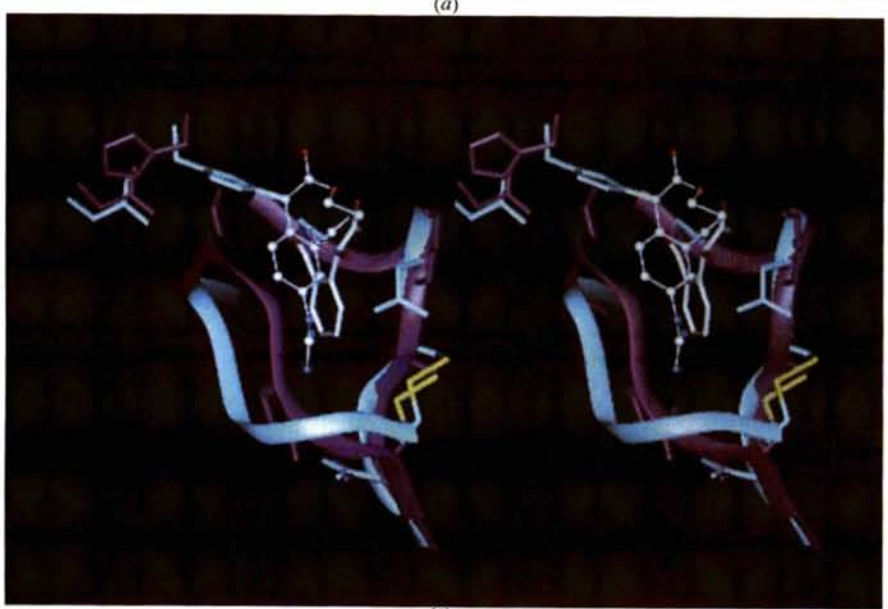

(*b*)

Fig. 3. (*a*) Stereo diagram of the inhibited active sites of factor D and trypsin. Factor D, magenta ribbon; DCI moiety, thick lines by atom colors; trypsin, gray ribbon; mono-covalently linked isocoumarin, ball-and-stick diagram by atom color. Diagram created using *QUANTA*96, (Molecular Simulations Inc.). (*b*) Stereo diagram of the inhibited active sites of factor D and trypsin. Factor D, magenta ribbon; DCI moiety, thick lines by atom colors; trypsin, gray ribbon; di-covalently linked isocoumarin, ball-and-stick diagram by atom color. Diagram created using *QUANTA*96, (Molecular Simulations Inc.).

pocket of **D**. In trypsin, residue 218 is a glycine, which allows the long positively charged amino-acid side chains of the natural substrates direct access to Asp189. In both the **D** and trypsin structures discussed. The carbonyl O atom of the inhibitor is directed away from the oxyanion hole. The remaining side chain of the two inhibitor molecules are almost superimposed, with the Cl atom situated near the α-hydroxyl position of DCI and the ester carbonyl O atom of the isocoumarin positioned near the carboxylate O atom of the DCI side chain. Both of these latter O atoms form hydrogen bonds to the peptide N atom of Gly193 in the oxyanion hole.

The second binding mode, a di-covalent linkage between trypsin and the substituted isocoumarin is not available to the **DCI:D** adduct. Although the DCI adduct initially held a Cl atom at the fourth position as did the trypsin:inhibitor complex (Fig. 3*b*), the orientation of this particular Cl atom is directed away from the active-site His57 residue as the lactone ring opens. The arched protein backbone of **D**, and in particular Ser215, must undergo dramatic changes in order to allow His57 to reorient itself into a position from which it could alkylate the side chain, displacing the Cl atom. This reorientation must occur for catalysis, but also must come at high energy costs, while the inhibitor and the His57 side chain have a significant amount of freedom in the trypsin active site. This double covalent linkage precludes the guanidinium group from penetrating as deep in the active site as above. The aromatic rings of the inhibitors now are near perpendicular, with the side chains oriented in different directions. The factor D pocket is narrow and restrained, preventing this type of rearrangement. Also, the carbonyl O atom of the trypsin adduct is now partially directed toward the oxyanion hole.

4.3. *Comparison of **DCI:D** with a benzoxazinone:elastase complex*

The structure of porcine pancreatic elastase bound to 5CL, a subsituted benzoxazinone (1inc, Radhakrishnan *et al.*, 1987), was chosen to show similarities between these types of complexes and **DCI:D**. The catalytic triad residues are in similar arrangements as were described in the trypsin and **D**-inhibited enzymes above (Fig. 4). The left-hand side of the active site, as viewed, reveals more dramatic changes in the basic architecture of the peptide backbone, while the right-hand side again proves to be nearly identical in conformation. As positioned, Val216 of the 5CL:PPE adduct fills a volume in the active site similar to that occupied by Arg218 (involved in the intramolecular salt bridges of **DCI:D**). The carbonyl O atoms of the respective inhibitors are nearly superposed, being directed away from the oxyanion hole. The O atom of the side-chain amide of 5CL:PPE is oriented in a similar manner to one of the carboxylate O atoms of the DCI moiety, forming a single hydrogen bond to the peptide N atom Gly193 in the oxyanion hole. This hydrogen bonding helps guide the side chain of 5CL:PPE towards the 'prime' specificity pockets of the elastase molecule.

4.4. *Discussion*

The structural comparisons of these inhibited trypsin and PPE enzymes with **DCI:D** proved further insight into the binding modes is possible between factor D and common serine protease inhibitors, striving towards the design of potent small-molecule pharmaceutical agents which can modulate the alternative complement pathway. The two isocoumarin-inhibited trypsin structures reaffirm the facts that several rearrangements must occur before other trypsin-like serine protease inhibi-

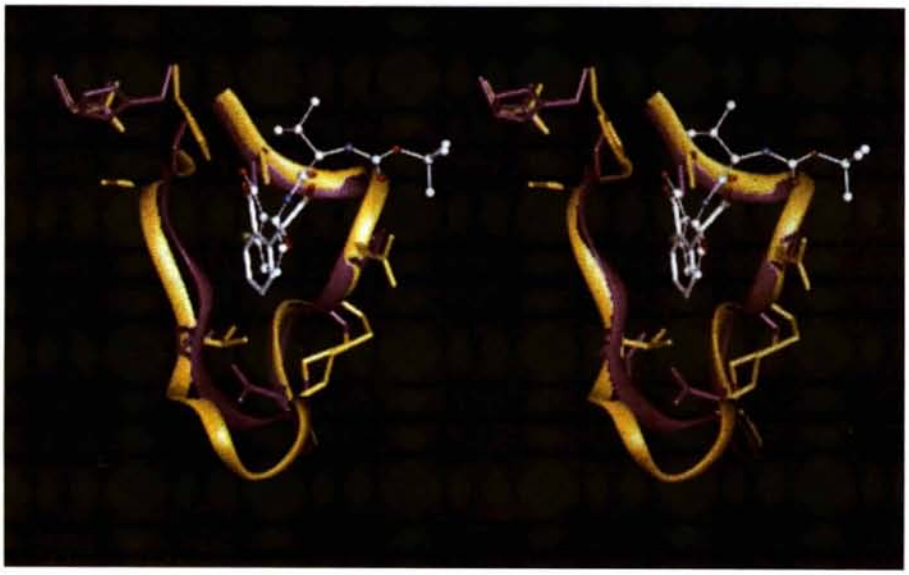

Fig. 4. Stereo diagram of the inhibited active sites of factor D and porcine pancreatic elastase. Factor D, magenta ribbon; DCI moiety, thick lines by atom colors; PPE, yellow ribbon; mono-covalently linked isocoumarin, ball-and-stick diagram by atom color. Diagram created using *QUANTA*96 (Molecular Simulations Inc.)

tors can inactivate **D**; not only must the short stretch of loop region including Ser215 shift, such that His57 can swing into the active conformation, but that the Arg218–Asp189 salt bridge in **D** must be completely disrupted. Although the main-chain similarities between the 5CL:PPE structure and **DCI:D** are fewer that those between the inhibited trypsin examples, the superpositioning of Val216 in 5CL:PPE over Arg218 in the **DCI:D** may suggest that small molecules similar to PPE inhibitors may provide key insights into future structure-based drug-design effects focusing on **D**. From these types of comparative studies, it is clear that either the salt bridge in **D** must be broken, or must be accounted for both sterically and electronically in the active site. The orientations of the side chains in these structures have indicated potential hydrogen-bonding networks that would direct groups toward the *S'* sites of the enzyme. Inhibitors which direct the carbonyl O atoms away from the oxyanion hole have a much greater stability in binding, yet is is unclear whether this is a requirement in the design of a potent **D** inhibitor, based upon the natural regulatory mechanisms of this complement protein. These comparison studies are continuing to provide key insights in the structure-based drug design of pharmaceutical agents capable of modulating the alternative complement pathway.

This work was supported by BioCryst Pharmaceuticals, Inc. and the NIH (SBIR grant 1-R43-AR41095-01). The authors would like to thank Dr John E. Volanakis of the Division of Clinical Immunology and Rheumatology, University of Alabama at Birmingham, for providing factor D used in the crystallization studies. Dr Edgar F. Meyer Jr of the Department of Biochemistry and Biophysics, Texas A & M University, for providing atomic coordinates for the isocoumarin: trypsin structures discussed. Dr Scott Rowland, BioCryst Pharmaceuticals, Inc., was very helpful in the preparation of the stereo figures and proofreading this manuscript.†

References

Barnum, S. R., Niemann, M. A., Kearney, J. F. & Volanakis, J. E. (1984). *J. Immunol. Methods*, **67**, 303–309.

Brünger, A. T. (1990). *Acta Cryst.* A**46**, 46–47

Brünger, A. T. (1992*a*). *X-PLOR: A System for X-ray Crystallography and NMR.* Version 3.1. New Haven and London: Yale University Press.

Brünger, A. T. (1992*b*). *Nature (London)*, **355**, 472–475.

Bugg, C. E., Carson, W. M. & Montgomery, J. A. (1993). *Sci. Am.* **296**(6), 92–98.

Chow, M. M., Meyer, E. F., Bode, W., Kam, C.-M., Radhakrishnan, R., Vijayalakshmi, J. & Powers, J. C. (1990). *J. Am. Chem. Soc.* **112**(21), 7783–7789.

Cole, L. B., Chu, N., Kilpatrick, J. M., Volanakis, J. E., Narayana, S. V. L. & Babu, Y. S. (1997). *Acta Cryst.* D**53**, 143–150.

Cryer, H. G., Richardson, J. D., Longmire-Cook, S. & Brown, C. M. (1989). *Arch. Surg.* **124**, 1378–1385.

Fearon, D. T., Austen, K. F. & Ruddy, S. (1974). *J. Exp. Med.* **139**, 355–366.

Hansson, G. K., Jonasson, L., Seifert, P. S. & Stemme, S. (1989). *Atherosclerosis*, **9**, 567–578.

Howard, A. J. Gilliland, G. L., Finzel, B. C., Poulos, T. L., Ohelendorf, D. H. & Salemme, F. R. (1987). *J. Appl. Cryst.* **20**, 383–387.

Jones, T. A. (1978). *J. Appl. Cryst.* **11**, 268–272.

Kam, C.-M., McRae, B. J., Harper, J. W., Niemann, M. A., Volanakis, J. E. & Powers, J. C. (1987). *J. Biol. Chem.* **262**, 3444–3451.

Kam, C.-M., Oglesby, T. J., Pangburn, M. K., Volanakis, J. E. & Powers, J. C. (1992). *J. Immunol.* **149**, 163–168.

Kerrigan, J. E., Oleksyszyn, J., Kam, C. M., Selzler, J. & Powers, J. C. (1995). *J. Med. Chem.* **38**, 544–552.

Kleywegt, G. J. & Brünger, A. T. (1996). *Structure*, **4**(8), 897–904.

Laskowski, R. A., MacArthur, M. W., Moss, D. S. & Thornton, J. M. (1993). *J. Appl. Cryst.* **26**, 283–291.

Lesavre, P. H., Hugli, T. E., Esser, A. F. & Muller-Eberhard, H. J. (1979). *J. Immunol.* **123**, 529–534.

Lesavre, P. H. & Muller-Eberhard, H. J. (1978). *J. Exp. Med.* **148**, 1498–1509.

Narayana, S. V. L., Carson, M., El-Kabbani, O., Kilpatrick, J. M., Moore, D., Chen, X., Bugg, C. E., Volanakis, J. E. & DeLucas, L. J. (1994). *J. Mol. Biol.* **235**, 695–708.

Nicholls, A., Sharp, K. A. & Honig, B. (1991). *Proteins*, **11**(4), 282–296.

Niemann, M. A., Bhown, A. S., Bennett, J. C. & Volanakis, J. E. (1984). *Biochemistry*, **23**, 2482–2486.

Powers, J. C. & Kam, C.-M. (1994). *Methods Enzymol.* **244**, 442–457.

Radhakrishnan, P., Presta, L. G., Meyer, E. F. Jr & Wildonger, R. (1987). *J. Mol. Biol.* **198**, 417–424.

Salvesen, N. G. & Nagase, H. (1989). *Proteolytic Enzymes, A Practical Approach*, edited by R. J. Beyon & J. A. Bond, pp. 83–104. New York: IRL Press.

Volanakis, J. E., Barnum, S. R. & Kilpatrick, J. M. (1993). *Methods Enzymol.* **223**, 82–97.

Volanakis, J. E. & Macon, K. J. (1987). *Anal. Biochem.* **163**, 242–246.

Yasuda, M., Takeuchi, K., Hiruma, M., Iida, H., Tahara, A., Itagane, H., Toda, I., Akioka, K., Teragaki, M., Oku, H., Kanayama, Y., Takeda, T., Kolb, W. P. & Tamerius, J. D. (1990). *Circulation*, **81**(1), 156–163.

† Atomic coordinates and structure factors have been deposited with the Protein Data Bank, Brookhaven National Laboratory (Reference: 1DIC). At the request of the authors, the atomic coordinates and structure factors will remain privileged until 1 July 1999.